SLAC-TN-15-048

Pulse Tube Interference in Cryogenic Sensor Resonant Circuits

Tyler Lam
SLAC National Accelerator Laboratory
August 2015

SLAC National Accelerator Laboratory, 2575 Sand Hill Road, Menlo Park, CA 94025

This material is based upon work supported by the U.S. Department of Energy, Office of Science, Office of Workforce Development for Teachers and Scientists (WDTS) under the Science Undergraduate Laboratory Internship (SULI) program, under Contract No. DE-AC02-76SF00515.

Abstract

Transition edge sensors (TES) are extremely sensitive superconducting sensors, operating at 100 mK, which can be used to detect X-rays and Cosmic Microwave Background. The goal of our project is to design the electronics to read out an array of 10000 of these sensors by using microwave signals. However, we noticed the pulse tube used to maintain cryogenic temperatures caused interference in our readout. To determine the cause of the signal distortions, we used a detector with a 370 MHz sampling rate to collect and analyze sensor data. Although this data provided little information towards the nature of the noise, it was determined through a maintenance procedure than the 0.3 mm stainless steel wires were being vibrated due to acoustic waves, which distorted the signal. Replacing this wire appeared to cease the interference from the sensor data.

I. INTRODUCTION

Improved detector sensitivity has benefits for a wide range of sciences. A more sensitive detector allows for more meaningful data to be taken from experimentation. Transition Edge Sensors (TES) are extremely sensitive superconducting energy detectors, capable of energy resolutions of 2.38 eV at 5.9 keV for X-rays and time resolution on the order of microseconds (Irwin and Hilton, 2005). Currently, these sensors have been used as detectors to measure the energy of X-rays; for example, they have been able to measure the energy of titanium*K*a fluorescence with a resolution of less than 14 eV full width at half-maximum (Irwin *et all* 1996). Using techniques proposed by Kent Irwin involving microwave multiplexing, we hope to read out an array of 10,000 sensors, which will be used as X-ray and cosmic microwave background detectors (Irwin and Hilton 2005). The long term goal of our group is to design and produce electronics to readout the data from the TES detectors.

In order to maintain the cryogenic temperature required by the TES, we used a pulse tube cryocooler to keep the system at 100 mK. The pulse tube functions using a piston to pump helium through a series of tubes and adiabatic chambers, and emits a very distinct, high pitched whistle, periodic on the order of 1-2 Hz. During early testing, we looked at the sensor data using a network analyzer and noticed interference and distortion of the signal which appeared and vanished in sync with the noise from the pulse tube.

To discover the cause of the interference, we first had to determine how the signal was being distorted. This paper will outline the methods used to interpret the data taken from the sensor, as well as a description of the system itself.

II. MATERIALS AND METHODS

A. Transition Edge Sensors

A TES functions by cooling a superconductor to its critical temperature, where the resistance begins to drop to zero, and running a current through the material by applying a bias voltage (Burney, 2006). A typical temperature vs. resistance curve for a superconducting material shows a gradual decrease in resistance, followed by a sharp roll off to zero as temperature decreases. The sharp drop occurs at the critical temperature and is known as the “Transition Edge”, where the material becomes superconducting. At this edge, any increase in temperature results in a significant increase in the resistance. The increased resistance lowers the current through the sensor, which drops the power through the superconductor. This drop in power lowers the temperature of the sensor back to its critical temperature. Figure 1 shows an example of the temperature response for a TES that has detected a particle.

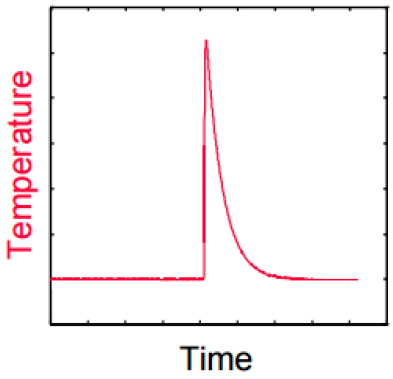

Fig. 1. *A TES that has detected an x-ray photon will show a sharp temperature increase at the detection, followed by decrease as the current is lowered.*

B. SQUIDs and Resonant Circuits

The current change in a transition edge sensor can be measured by connecting an inductance loop to the circuit and inductively coupling a Superconducting Quantum Interference Device (SQUID) to the inductance loop. A SQUID is a ring of superconducting material used as an amplifier for magnetic flux (Van Duzer and Turner, 1981). When current through the inductance loop changes, mutual inductance causes a change in magnetic flux through the SQUID. The SQUID then creates current dependent on the magnitude of the change in flux.

Reading out this change in SQUID current relies on the use of resonant circuits. Figure 2 and the equations below show the impedance response of an RLC "Tank" circuit:

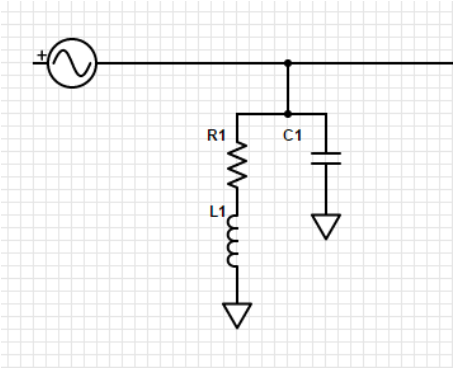

Fig. 2. *Circuit consisting of an inductor in series with a resistor, all in parallel with a capacitor*

$$Z_{lc} = (Z_r + Z_l)||Z_c \tag{1}$$

$$Z_{lc} = \frac{(R + i\omega L)\left(\frac{1}{i\omega C}\right)}{R + i\omega L + \frac{1}{i\omega C}} \tag{2}$$

$$Z_{lc} = \frac{R + i[\omega L(1 - \omega^2 LC) - \omega R^2 C]}{(R\omega C)^2 + [\omega^2 LC - 1]^2} \tag{3}$$

Setting the imaginary part of the impedance to zero and solving for ω gives us the resonant frequency. A resonant circuit driven at this frequency acts as a short; the impedances reaches its maximum value while the transmitted power reaches a minimum. We can measure the resonant frequency by driving broadband noise through the circuit, measuring the transmitted power for each frequency, and finding the minimum value. Figure 3 shows the transmitted power vs. frequency for a circuit with a quality factor (Q-factor) of 20. The circuits present in the sensors have a quality factor on the order of 10^5, yielding a much narrower dip relative to the resonant frequency of the circuit.

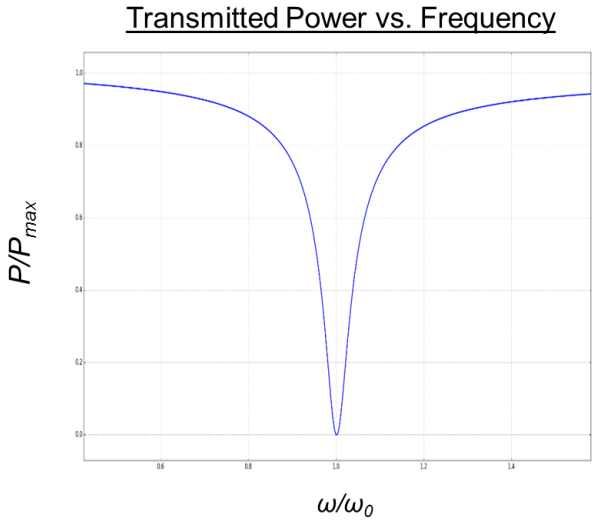

Fig. 3. *An RLC resonant circuit experiences a sharp drop in transmitted power when driven at resonance*

The SQUID is coupled to the resonant circuit, which causes the resonant frequency of the RLC circuit to shift when a change in magnetic flux is detected (Gallop, 1991). This shift in RLC circuit is proportional to the change in magnetic flux, which is proportional to the energy of a

particle detected by the TES. Sweeping continuous broadband noise through the RLC circuit allows us to measure the change in resonant frequency by tracking the frequency with the lowest transmitted power, and determine the energy of the particle detected.

C. Measuring Pulse Tube Interference

A network analyzer measures the response to a range of frequencies by sending one frequency at a time through the system and measuring the response. While using this to measure the resonance dips in the sensor, we noticed significant distortion and interference, as seen in figure 4. Moreover, when looking at the broadband frequency response, we observed the dips getting wider and narrower in sync with the pulse tube noise. Due to the lower sampling rate of the scope, we were unable to determine the nature of the interference; one possibility is the peaks could have actually been changing shape due to a change in the Q-factor of the resonant circuit, another is the actual resonance itself shifted and was being aliased. In order to determine exactly how the resonance peaks were shifting, we used a Texas Instruments ADC16DX370 analog to digital converter (ADC) with a sampling rate of 370 MHz to collect sensor data and track resonances over time. The digital to analog converter (DAC) which creates the signal and the ADC function in the microwave frequency, while the resonant frequencies of the sensor are around 5 GHz. In order to convert these signals to the proper range, Dan Van Winkle and Mark Petree designed and created an up/down conversion box consisting of several mixers, filters, and amplifiers.

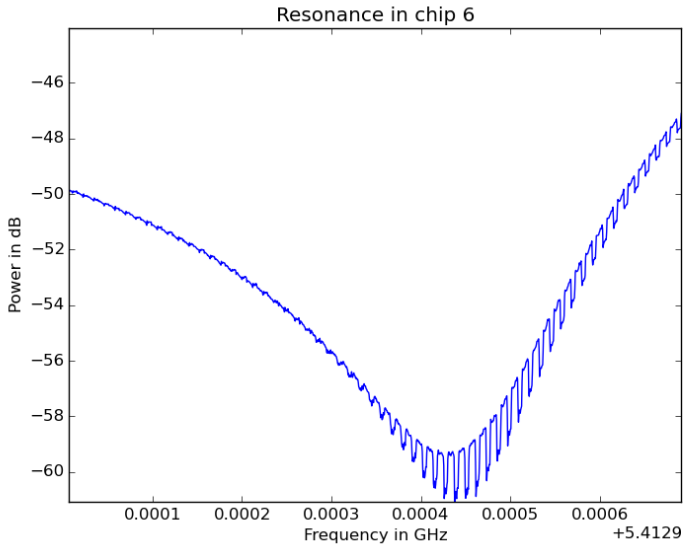

Fig. 4. *A resonant dip being distorted by the pulse tube*

To track several resonances at once, we drove broadband noise through the sensor, and compared the frequency response of the signal in to the signal out. This noise was periodic to 2^{16} bins, or about 0.1772 milliseconds, driven with a trigger signal that marked the beginning and end of each block. Taking the Fourier transform of each block allowed us to compare the corresponding frequency response. In order to determine if the pulse tube noise was on during the data collection, we aimed a camera at the "collect" button and filmed the moment the data was collected. Slowing down the video and amplifying the sound allowed us to match the moment of data collection to the sound of the pulse tube, and label the data collected as "on" if the noise was present, or "off" if the noise was absent.

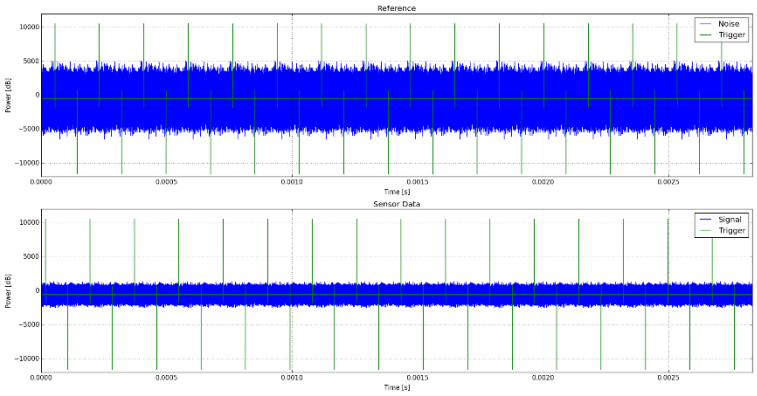

Fig. 5.1. *(Top) Reference data, taken without being sent through sensor*

Fig 5.2. *(Bottom) Signal data taken by driving reference through sensor*

We took a data sample that was 2^{24} bins long at 370 Hz, equaling 16777216 data points over 0.04534 seconds. The data in the time domain can be seen in figure 5 above. To trace the resonances over time, we created a Waterfall Fourier Transform for each resonant frequency. This was done by taking the Fourier transform of each block of reference and sensor data to get our data in the frequency domain, smoothing the data by using a rolling average, then taking the ratio of the power of the signal to the reference. We then zoomed in on each resonance dip and created a heat plot corresponding to the power level in dBF. This process was repeated for each of the noise blocks, which were then stacked in chronological order to determine any possible changes in the resonance shape.

III. RESULTS

We collected 20 sets of data, with an even split between having the pulse on and off. The Fourier Transform showed several clear resonance peaks, as seen in figure 6; we chose to analyze the cleaner resonances spanning from 136 MHz to 160 MHz.

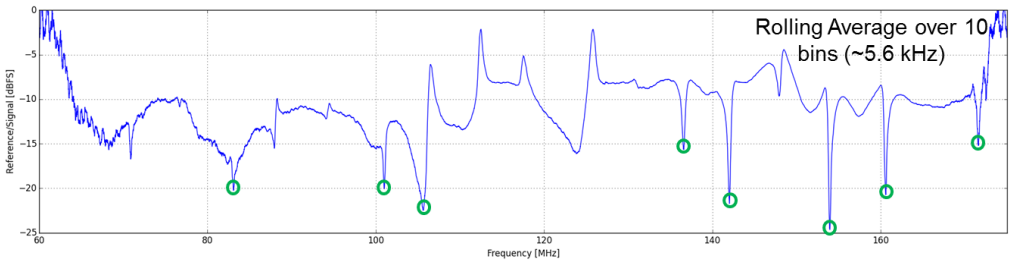

Fig. 6. *Resulting power from dividing the reference data to the sensor data. Resonance dips are circled*

The Waterfall Fourier Transforms showed very little variation. Slight widening and narrowing was observed, although neither consistently corresponded to having the pulse tube on or off. Additionally, the resonance dips did not show any noticeable difference or shifting from the initial resonant frequency. Qualitatively, very little signs of interference can be obtained from these plots. Figures 7 and 8 show several resonance traces for 154.01 MHz, with the x-axis in MHz, y-axis in seconds, and color in dBF.

We were able to check our measurement techniques by using a flux ramp, which drives flux through the SQUID in order to manually shift the resonant frequency. We determined that the analysis techniques were sensitive enough to resolve down to significantly less than one Full Width at Half Maximum (FWHM) of the resonance dip, as seen in figure 9, and supported the lack of difference between the waterfall Fourier transforms.

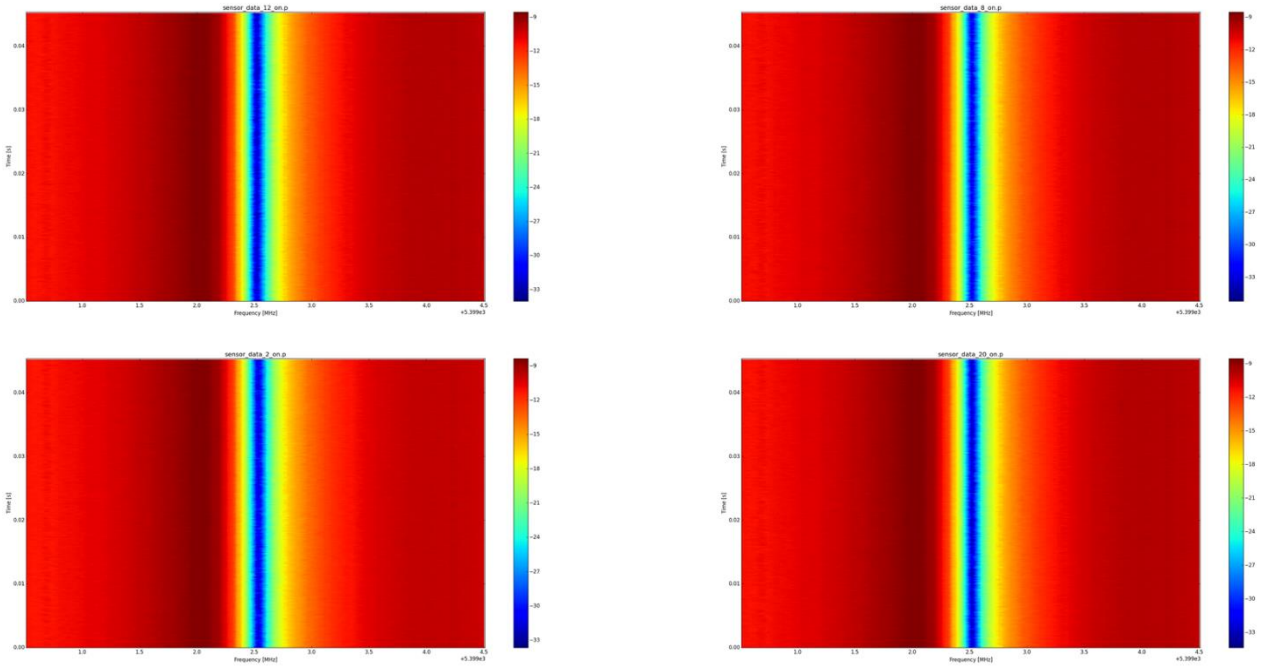

Fig. 7. *Waterfall Fourier Transform with pulse tube noise on*

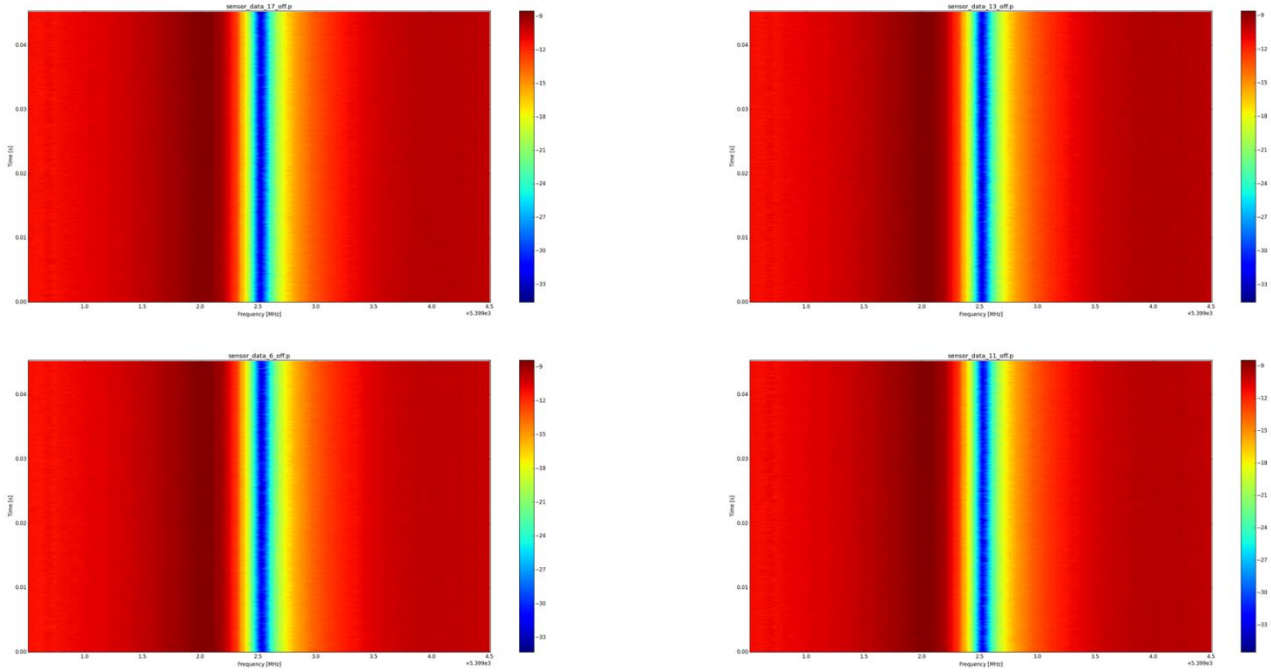

Fig. 8. *Waterfall Fourier Transform with pulse tube noise off*

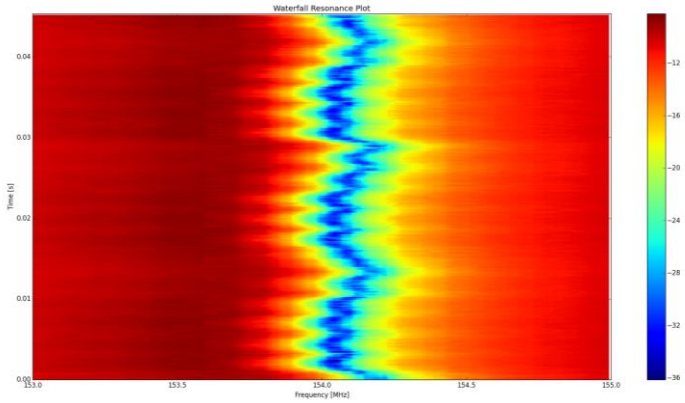

Fig. 9. *Resonance dip being manually shifted by a flux ramp*

To analyze the resonant behavior of the sensor, we calculated the resonant frequency (after down converting to the digitizer range) for each resonance dip by finding the frequency at which the lowest power level occurred for each time period in the Waterfall Fourier Transform. One possibility for this interference would be a rapid shift in the resonant frequency- if so, either the data taken with the pulse tube on or off would show a higher standard deviation. If the shifting in resonant frequency was slower, it could show a change in the average resonant frequency as well as the standard deviation.

	Resonance [MHz]	**Standard Dev.**	**Resonance [MHz]**	**Standard Dev.**	**Resonance [MHz]**	**Standard Dev.**
Off	154.012	0.0021	160.7	0.55	142.1	1.43
On	154.011	0.0015	160.7	0.53	142.1	1.36

	Resonance [MHz]	**Standard Dev.**	**Resonance [MHz]**	**Standard Dev.**
Off	136.7	1.58	148.053	0.0068
On	136.7	1.59	148.053	0.0066

Although the standard deviation in general was larger for the pulse tube off, it is neither consistent and nor significant enough to be statistically meaningful. This led us to believe that there was no aliasing in the spectrum analyzer, and the shape of the resonance itself may have been changing between the pulse tube on and off. Each resonant peak for on and off was averaged in order to determine if the overall shape or depth of the resonance varied. These averages can be seen in figure 10.

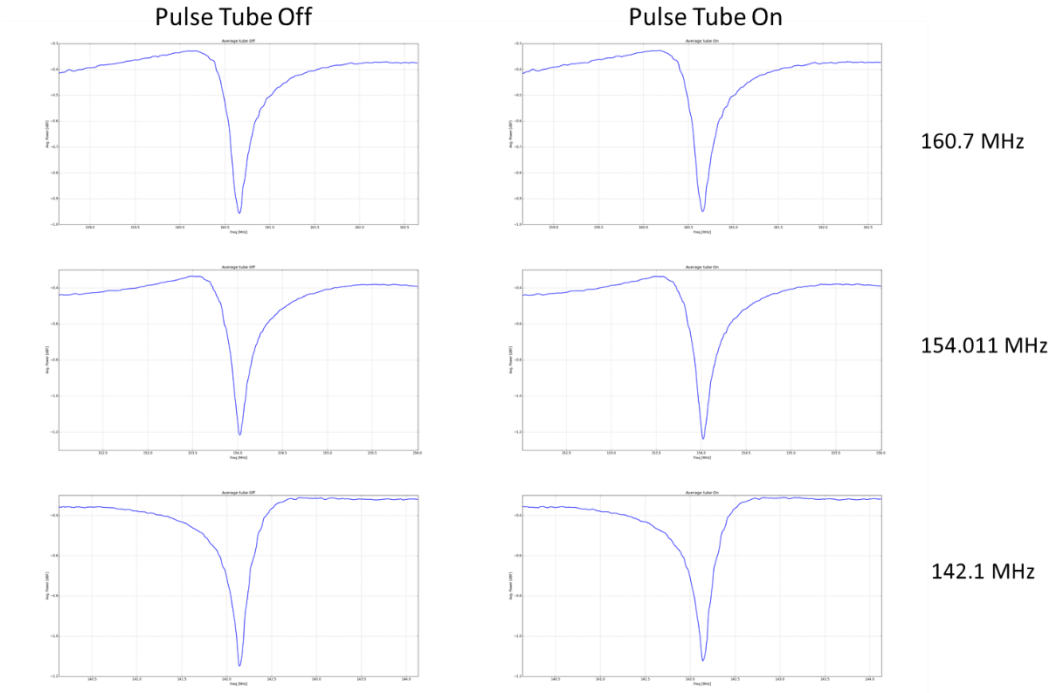

Fig. 10. *Averaged resonant dips for pulse tube on and off*

Despite the small differences between the two averages, none are consistent enough to show any meaningful changes. For example, the depth of the resonance is slightly lower for the pulse tube off in the 142.1 MHz resonance, but higher for the 154.011 MHz resonance, while the resonance depth at 160.7 MHz barely changes at all. There appeared to be no difference in the width of the resonance between having the pulse tube on and off.

We also plotted the phase of the resonance as a function of time in hopes of finding some irregularity that may indicate anything interfering in the sensor. However, there was yet again no sign of differences between phase for the pulse tube on and off, as can be seen in figure 11.

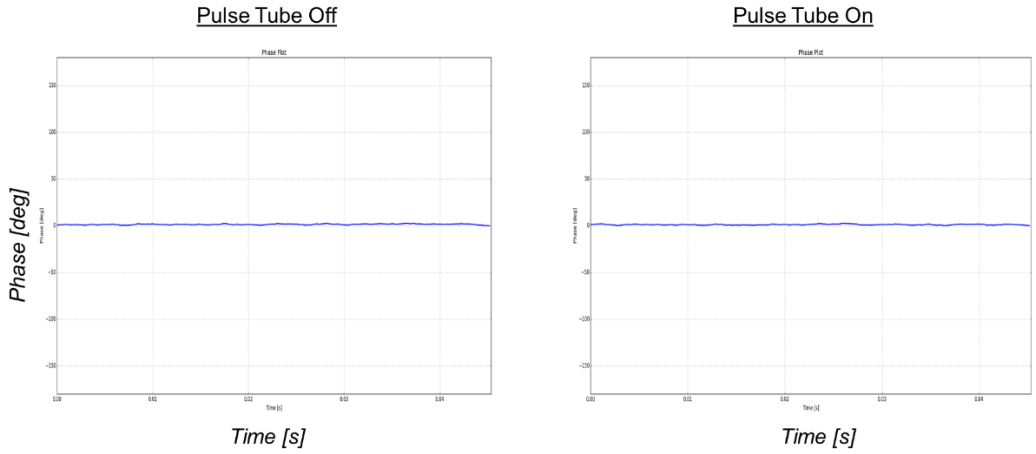

Fig. 11. *Phase versus time for the pulse tube on and off*

IV. DISCUSSION AND CONCLUSIONS

The data we collected showed very little as to the nature of the pulse tube noise. Interference was clearly shown on both our scopes and the spectrum analyzer, yet was absent in the data collected by the 370 MHz analog to digital converter. We observed neither a shift in the resonant frequency nor a change in the quality factor of the system. Nothing in the data suggests

interference from the pulse tube of any kind. Based on the data, we can draw no conclusions about the cause of the interference or any possible solution.

During the process of analyzing the data, the sensor was warmed up to replace parts. One of which was 0.3 mm stainless steel wire running through the cryocooler. Once replaced with thicker, sturdier wire, the pulse tube noise vanished, on both the spectrum analyzer and the scopes measuring broadband noise. We believe that the cause of the noise was a physical vibration affecting the signal through the wire, which was caused by the pulse tube piston. Previous experiments involving manually tapping the system have shown that physical vibrations can affect the frequency response, as shown in figure 12.

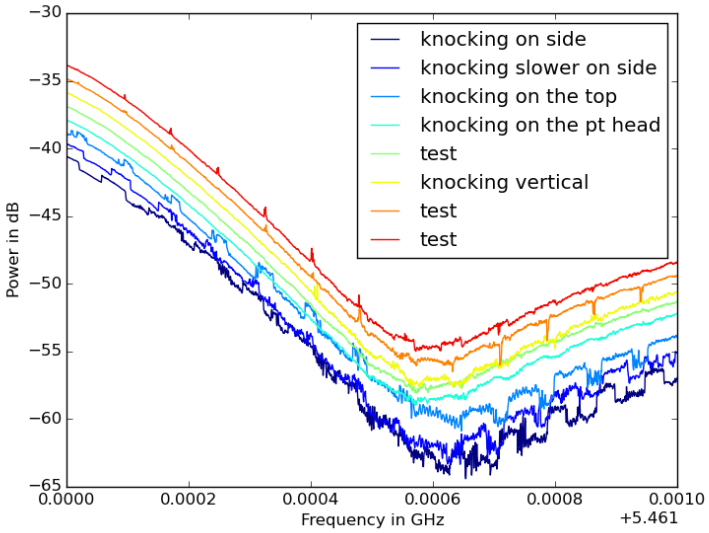

Fig. 12. *Physical vibrations can cause additional noise in the cryogenic system*

In summary, we noticed interference in the resonant circuit response which occurred in sync with the acoustic noise from the pulse tube used to cool the sensor. This noise was first observed using a network analyzer and through looking at the broadband response through a scope. In order to determine the cause of this noise, we drove broadband noise created from a digitizer in

the microwave range through an up/down conversion box measure the sensor response, and a 370 MHz analog to digital converter to collect data and track the resonant dips over time. No sign of interference was found on the data collected, although the techniques were enough to resolve a shift down to one FWHM. Replacing the 0.3 mm stainless steel cables appeared to stop the pulse tube interference, most likely minimizing the impact of physical vibrations. However, further experimentation is required to determine why the noise was visible on the spectrum analyzer and not on the data taken with the ADC.

V. ACKNOWLEDGEMENTS

I would like to acknowledge my mentor, Josef Frisch, Dan Van Winkle, and Sarah Kernasovskiy for being extraordinarily helpful throughout this internship. They have all taught me an incredible amount and I thank them for providing me research experience this summer. I would also like to acknowledge Enrique Cuellar, Maria Mastrokyriakos, and the Department of Energy for making this program possible.

Bibliography

Burney, Jennifer A. "Transition-Edge Sensor Imaging Arrays for Astrophysics Applications." Thesis. Stanford University, 2006. Print.

Chervenak, J. A., K. D. Irwin, E. N. Grossman, John M. Martinis, C. D. Reintsema, and M. E. Huber. "Superconducting Multiplexer for Arrays of Transition Edge Sensors." *Appl. Phys. Lett. Applied Physics Letters* 74.26 (1999): 4043. Web.

Gallop, J. C. "Resonant Detection System." SQUIDS, the Josephson Effects and Superconducting Electronics. Bristol, England: Adam Hilger, 1991. N. pag. Print.

Irwin, Kent D. "Transition Edge Sensors." Cryogneic Particle Detection. By Gene C. Hilton. Ed. Hans-Christian Stahl. 1st ed. Vol. 99. Berlin: Springer-Verlag, 2005. 63-149. Print.

Irwin, K. D., G. C. Hilton, D. A. Wollman, and John M. Martinis. "X-ray Detection Using a Superconducting Transition-edge Sensor Microcalorimeter with Electrothermal Feedback." *Appl. Phys. Lett. Applied Physics Letters* 69.13 (1996): 1945. Web.

Van Duzer, T. and Turner, C.W., *Principles of Superconductive Devices and Circuits*, Elsevier, New York (1981)

"Transition Edge Sensors." *MIT Experimental Cosmology and Astrophysics Laboratory*. Figueroa Group, n.d. Web. 19 Aug. 2015.